Anal. Chem. **2006,** *78,* 3282−3288

Gold and Silica-Coated Gold Nanoparticles as Thermographic Labels for DNA Detection

Marta G. Cerruti,† Marc Sauthier,† Donovan Leonard,‡ Dage Liu,† Gerard Duscher,‡ Daniel L. Feldheim,*,† and Stefan Franzen*,†

Department of Chemistry, North Carolina State University, Raleigh, North Carolina 27695, and Department of Material Science, North Carolina State University, Raleigh, North Carolina 27695

The infrared emissivity of Au and silica-coated Au nanoparticles (Au NPs) deposited on indium tin oxide substrates was investigated. NPs were irradiated with laser light at a frequency close to the Au plasmon resonance band, and the blackbody radiation emitted as a result was monitored with an IR camera equipped with an InAs array detector. The differences in temperature before and after laser irradiation were recorded (*T*-jumps) and were found to be directly proportional to the number of particles present on the slide and to the laser power used in the experiment. Coating Au NPs with silica increased the measured *T*-jumps 2−5 times, depending on the thickness of the silica shell. This was in agreement with the observation that silica has a much higher IR emissivity than Au. Both Au and silica-coated Au NPs were then tested as labels for thermographic DNA detection. Target DNA concentrations as low as 100 pM were recorded when Au NPs were used as labels and as low as 10 pM when silica-coated Au NPs were used.

The visible light extinction properties of gold nanoparticles (Au NPs) have been exploited for many centuries. Perhaps the first use of Au NPs was as pigments in paint and glass, as demonstrated by the Lycurgus cup, a Roman artifact dating back to the 4th century. Despite their long history, an understanding of the physical origins of light extinction by Au NPs was not achieved to a high level until the mid-1800s to early 1900s when Faraday, Maxwell-Garnett, Mie, and others began their pioneering work in the field.[1] Mie first solved Maxwell's equations to calculate the extinction spectra of spheres, and many theoretical, and experimental advances have followed which have enabled a deeper understanding of light extinction mechanisms by nonspherical particles (e.g., spherical aggregates, rods, prisms, etc.).[2−7]

Recently, photophysical studies of metal particles have expanded beyond light extinction. Au NPs have been shown to possess large first-order hyperpolarizabilities,[8,9] enhance Raman scattering signals from molecular adsorbates,[10] and fluoresce with moderate quantum yields.[11] It has also been shown that the visible light extinctions of Au NPs relax thermally to heat their surroundings. For 10-nm-diameter Au NPs, the peak of the plasmon absorption occurs at 520 nm, which is reasonably well matched to a Nd:YAG excitation source at 532 nm. Heat emitted by Au NPs can be exploited to affect electrochemical behaviors,[12] induce gel polymer phase transitions,[13,14] and to thermally ablate tumor cells.[15] Here, the blackbody radiation emitted from Au NPs in response to plasmon excitation was exploited to create labels for sensing applications. In particular, Au NPs were used to detect the hybridization of a single-stranded DNA (ssDNA) sequence in solution to a complementary ssDNA sequence on a surface. Fluorescence has been widely used as a method for detecting DNA hybridization and protein binding in an array format. The present study uses DNA hybridization as a model system to explore the use of robust labels that do not degrade, quench, or photobleach.

The presence of hybridized double-stranded DNA (dsDNA) was detected by thermal emission produced by laser excitation of the Au NPs at their plasmon frequency. The detection of thermal emission from nanoparticles requires that the detector be matched approximately to the blackbody temperature of the emitting particle. According to the Wien displacement law, $\lambda_{max}T = 2.88 \times 10^6$ nm-K; thus, at 288 K, the wavelength is 10^4 nm or

* Address correspondence to either author. E-mails: Dan_Feldheim@NCSU.edu, Stefan_Franzen@NCSU.edu.

† Department of Chemistry.

‡ Department of Material Science.

(1) Foss, C. A. Jr.; Feldheim D. L. In *Me*tal Nanoparticles: Synthesis, Characterization and Applications; Foss, C. A., Jr., Feldheim D. L., Eds.; Marcel Dekker: New York, 2002.

(2) Hicks, E. M.; Zhang, X. Y.; Zou, S. L.; Lyandres, O.; Spears, K. G.; Schatz, G. C.; Van Duyne, R. P. *J. Phys. Chem. B* **2005**, *109*, 22351−22358.

(3) Pinchuk, A.; Schatz, G. *Nanotechnology* **2005**, *16*, 2209−2217.

(4) Shuford, K. L.; Ratner, M. A.; Schatz, G. C. *J. Chem. Phys.* **2005**, *123*, 114713.

(5) El-Kouedi, M.; Foss, C. A. *J. Phys. Chem. B* **2000**, *104*, 4031−4037.

(6) Foss, C. A.; Hornyak, G. L.; Stockert, J. A.; Martin, C. R. *J. Phys. Chem.* **1994**, *98*, 2963−2971.

(7) Douketis, C.; Haslett, T. L.; Wang, Z.; Moskovitis, M.; Iannotta, S. *J. Chem. Phys.* **2000**, *113*, 11315−11323.

(8) Kim, Y.; Johnson, R. C.; Li, J.; Hupp, J. T.; Schatz G. C. *Chem. Phys. Lett.* **2002**, *352*, 421−428.

(9) Novak, J. P.; Brousseau, L. C., III; Vance, F. W.; Johnson, R. C.; Lemon, B. I.; Hupp, J. T.; Feldheim, D. L. *J. Am. Chem. Soc.* **2000**, *122*, 12029−12030.

(10) Orendorff, C. J.; Gole, A.; Sau, T. K.; Murphy, C. J. *Anal.* Chem. **2005**, *77*, 3261−3266.

(11) Huang, T.; Murray, R. W. *J. Phys. Chem. B* **2001**, *105*, 12498.

(12) Lowe, L. B.; Brewer, S. H.; Kramer, S.; Fuierer, R. R.; Qian, G.; Agbasi-Porter, C. O.; Moses, S.; Franzen, S.; Feldheim, D. L. *J. Am. Chem. Soc.* **2003**, *125*, 14258−14259.

(13) Mohamed, M. B.; Ahmadi, T. S.; Link, S.; Braun, M.; El-Sayed M. A. *Chem. Phys. Lett.* **2001**, *343*, 55−63.

(14) Kim, J.; Serpe, M. J.; Lyon L. A. *Angew.* Chem., Int. Ed. **2005**, *44*, 1333−1336.

(15) Hirsch, L. R.; Jackson, J. B.; Lee, A.; Halas, N. J.; West, J. L. *Anal. Chem.* **2003**, *75*, 2377−2381.

10.1021/ac0600555 CCC: $33.50
Published on Web 04/20/2006

10 μm. The InAs array detector is an imager with a peak response near 10 μm (1000 cm^{-1}) in the mid-infrared range. This is a sensitive detector that can resolve even small differences in the emissivity of materials in the mid-infrared range. In the current application, the sensitive detection of nanoparticle heating is demonstrated. There are actually two effects of increasing the temperature by laser-induced heating of Au NPs by excitation of the plasmon band. First, there is a small wavelength shift according to the Wien law. However, the second effect is a large increase in emitted intensity with temperature. The sensitivity of the thermographic detection method is largely due to the flux dependence of emitted radiation according to the Stefan−Boltzmann equation, $W = \sigma T^4$, where W is the emitted flux, T is temperature, and σ is the Stefan−Boltzmann constant. The intensity is modulated by the emissivity of the particle, which is quite different for a conductor (gold) and an insulator (silicon dioxide). The emissivities of Au and Au−silica core−shell particles in the mid-infrared range were compared in this study to demonstrate this effect. The intensity of blackbody radiation emitted by Au−silica core−shell NPs was increased relative to Au NPs due to the high emissivity of silica in the mid-infrared range. When used as labels for DNA detection, silica-coated Au NPs improved detection limits by an order-of-magnitude compared to bare Au NPs.

MATERIALS AND METHODS

Chemical Modification of ITO. ITO slides (Delta Technologies, Ltd.) were composed of 90% indium oxide and 10% tin oxide and had a nominal thickness of 1500 Å and a sheet resistance of 8−12 Ω. A number of studies were carried out in the past concerning DNA binding on ITO.[16−19] The strategy used in the present paper to attach ssDNA on the ITO film was similar to that proposed by Moses et al.[20] However, instead of using 12-phosphododecanoic acid to modify the ITO surface as reported previously, 1,11-undecanedicarboxylic acid (UDA) (Sigma-Aldrich) was used.[21]

ITO slides were cut in 1 cm^2 squares and cleaned with UV−ozoneolysis (UVO) for 15 min (UVO cleaner (UVO-60), model number 42, Jelight Company, Inc). The slides were immersed overnight in a 4 mM solution of UDA, using a mixture of diethylamine/ethanol/H_2O (0.1/0.45/0.45 volume ratio) as solvent. The slides were then rinsed with H_2O and dried at 37 °C for 10 min.

Single-Stranded DNA (ssDNA) Attachment to UDA-Modified ITO. 5′-NH_2-modified ssDNA was purchased from MWG (the amino modifier was a $C_6H_{12}NH_2$ group). ITO slides were immersed in 900 μL of a 0.1 M MES (2-(*N*-morpholino)ethane sulfonic acid) buffer solution (pH 5) containing 1 μM of the amino-modified ssDNA and 200 mM EDC (1-ethyl-3-(3-dimethylaminopropyl)-carbodiimide hydrochloride, Sigma-Aldrich) for 4 h. This reaction is shown in Scheme 1. Two different sequences of DNA were used for the direct assay and the sandwich assay, as summarized in Table 1. The surface was then rinsed with H_2O and dried under the same conditions described above.

Scheme 1. Illustration of ssDNA attachment to ITO using UDA

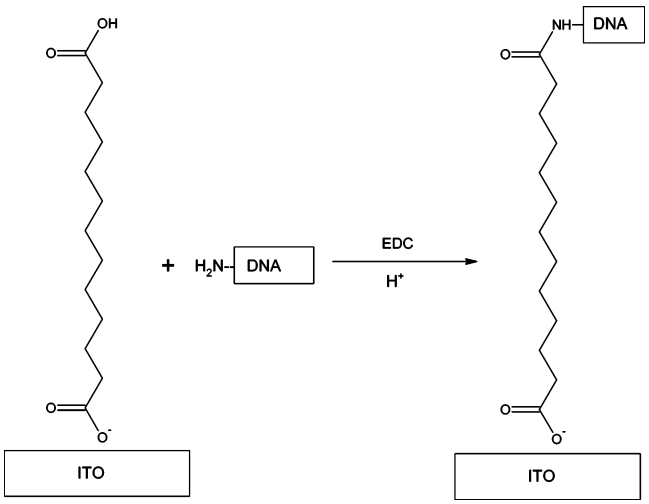

Synthesis of ssDNA-Modified Au Nanoparticle Tags. Au NPs were modified with an excess of thiol-terminated ssDNA (HS-DNA, purchased from MWG) following the procedure described by Demers and co-workers.[22] In a typical preparation, 1 mL of 9.4 nM citrate-coated Au NPs (10-nm-diameter, Ted Pella) was mixed with 1.5 mL of 3 μM HS-DNA. After 24 h, a solution of NaCl was slowly added, up to a final concentration of 0.1 M. The DNA-modified Au NPs were left stirring for an additional 48 h. The particles were centrifuged and washed with a mixture of 0.03 M NaCl/0.01 M phosphate buffer (pH 7) to remove excess unbound DNA. This procedure was repeated twice.

Preparation of Silica-Coated Au Nanoparticles. Silica-coated Au NPs were prepared following a procedure similar to that proposed by Lu et al.[23] TES (tetraethyl orthosilicate, Sigma Aldrich) was added to 10-nm-diameter, citrate-coated Au NPs (9.4 nM, Ted Pella), and NH_4OH (Sigma Aldrich) was used as a catalyst for the hydrolysis and recondensation of SiOH groups. The reaction was carried out in 2-propanol (Fisher). The amounts of TES/Au/NH_4OH/propanol varied and are reported in Table 2. After 1 h of stirring, the solution was centrifuged at 4000 rpm for 1 h (MiniSpin Plus, Eppendorf), and the particles were resuspended in water up to a final concentration of 5 nM.

The protocols described above frequently led to core−shell particles containing multiple Au particle cores per silica shell. To decrease the number of Au cores per particle, Au particles were stabilized with ligands prior to encapsulation with silica. MUA (mercaptoundecanoic acid, Sigma-Aldrich), MHA (mercaptohexadecanoic acid, Sigma-Aldrich), and BSPP were tested as ligand stabilizers. MUA and MHA attachment was accomplished by adding 5 mL of 10 mM solutions of MUA or MHA to 5 mL of Au NPs and stirring overnight. BSPP attachment was performed following the procedure described by Sauthier.[24] Micrographs of

(16) Yang, I. V.; Thorp, H. H. *Anal. Chem.* **2001**, *73*, 5316−5322.
(17) Armistead, P. M.; Thorp, H. H. *Anal. Chem.* **2000**, *72*, 3764−3770.
(18) Cai, H.; Shang, C.; Hsinga, I.-M. *Anal. Chim. Acta* **2004**, *523*, 61−68.
(19) Su, H.-J.; Surrey, S.; McKenzie, S. E.; Fortina, P.; Graves, D. J. *Electrophoresis* **2002**, *23*, 1551−1557.
(20) Moses, S.; Brewer, S. H.; Kraemer, S.; Fuierer, R. R.; Sauthier, M.; Lowe, L. B.; Agbasi, C.; Feldheim, D.; Franzen, S. *Langmuir* **2005**, in press.
(21) Napier, M. E.; Thorp, H. H. *Langmuir* **1997**, *13*, 6342−6344.
(22) Demers, L. M.; Mirkin, C. A.; Mucic, R. C.; Reynolds, R. A.; Letsinger, R. L.; Elghanian, R.; Viswanadham, G. *Anal. Chem.* **2000**, *72*, 5535−5541.
(23) Lu, Y.; Yin, Y.; Li, Z.-Y.; Xia, Y. *Nano Lett.* **2002**, *2*, 785−788.
(24) Sauthier, M. Development, characterization, and optimization of a Nanoparticle-based DNA hybridization detection strategy. In *Chemistry*; North Carolina State University: Raleigh, NC, 2001.

Table 1. DNA Abbreviations and Sequences Used in the Experiments Shown in the Paper

assay	DNA	sequence	identification
direct	U20	5′-H_2N-GTGAGCGGATAATCCTGGTT-3′	probe (on ITO)
	X20	5′-HS-AACCAGGATTATCCGCTCAC-3′	target (on Au)
sandwich	R15B	5′CTCACAATTCCACAC−NH_2−3′	probe (on ITO)
	R15A	5′-HS-GGAGACTGTTATCCG-3′	probe (on Au)
	S30	5′-GTGTGGAATTGTGAGCGGATAACAGTCTCC-3′	target

Table 2. Reactants Used to Prepare Silica-coated Au Nanoparticles

sample	Au10 9.4 nM mL	stabilizer	TES μL	NH_4OH mL	propanol mL	H_2O mL
TES10	1		10	0.125	5	
TES20	1		20	0.125	5	
TES40	1		40	0.125	5	
A	1	MHA	5	0.125	5	
B	1	BSPP	5	0.125	5	
C	0.5	MUA	30	0.25	10	1.5

the resulting particles are shown in Figure 1. Particle morphology, number of Au NP cores and shell thickness were determined from the TEM brightfield images. Single core particles, producing dark diffraction contrast, were observed more frequently in sample A (Figure 1a), and multiple Au NP cores were more frequent in samples B and C (Figure 1b and c). Confirmation of stoichiometric silica, chemical, and electronic property analysis of the silica-coated Au NPs from a combined scanning TEM (STEM) and electron energy loss spectroscopy (EELS) study will be reported in a forthcoming paper.

Modification of Silica-Coated Au Nanoparticles with HS-DNA. Single-stranded DNA probe oligonucleotides were attached to silica-coated Au NPs by first functionalizing the particles with (3-aminopropyl)trimethoxysilane (APS, Sigma-Aldrich). This was accomplished by combining 1 mL of 5 nM silica-coated Au particles with 5 μL of APS, 1 mM, for 1 h.

In a separate reaction, 1.5 mL of 5′-thiolated DNA (R15A, 3 μM) was reacted with 1 mg of sulfosuccinimidyl-4-*N*-maleimidomethyl cyclohexane-1-carboxylate (SSMCC, Pierce) in 1.5 mL of 0.05 M KP buffer (KP buffer was prepared by mixing 0.05 M solutions of KH_2PO_4 and $KHPO_4$, both purchased from Sigma Aldrich, until a final pH of 7.4 was reached). After 1 h, the DNA was separated from the excess SSMCC by centrifugation, using a 3000 molecular weight cutoff filter (Centricon, Millipore Corp.) and centrifuging at 14 000 rpm for 20 min.

The resulting purified, SSMCC-activated DNA was added to the NH_2-functionalized silica-coated Au particles and stirred for 2 h. The resulting particles were centrifuged at 4000 rpm for 1 h and resuspended in water up to a final concentration of 5 nM.

Au Nanoparticle Attachment on Poly-L-lysine-Coated ITO. ITO was first coated with a thin layer of poly-L-lysine (Sigma-Aldrich, molecular weight 4000−15 000). This was accomplished by UVO-cleaning ITO slides for 15 min, followed by immersion in a 1 mg/mL solution of poly-L-lysine for 1 h. The slides were then rinsed with water, dried with N_2, and immersed in 0.5 nM citrate-coated Au nanoparticle solution (20 nm in diameter, Ted Pella) for different amounts of time (5, 15, 30 min). The slides were then rinsed again in water and dried with N_2.

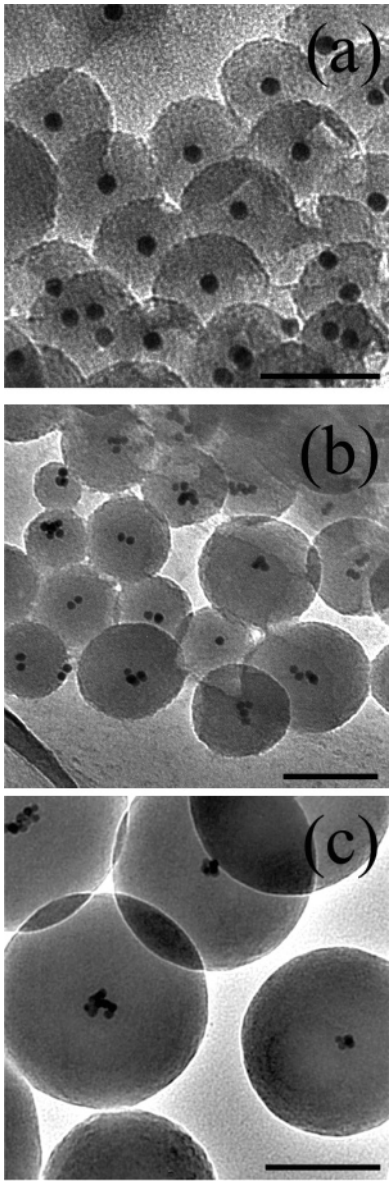

Figure 1. Transmission electron microscope images of silica-coated Au NP samples A, B, and C corresponding to images (a), (b), and (c), respectively. See Table 2 for information about particle synthesis procedures. Scale bars are 50 (a), 100 (b), and 150 nm (c).

IR Thermography Detection. Laser light at 532 nm produced with a coherent Verdi V-10 CW laser was used to irradiate the ITO slides. The laser beam was focused on a spot with a diameter of 0.7 mm. The changes in temperature were monitored using an SC3000 ThermaCAM (FLIR systems), which was equipped with a GaAs IR photodetector with a spectral range of 8−9 μm. The camera was interfaced to a computer using ThermaCAM Researcher software. The *T*-jumps were obtained as a difference

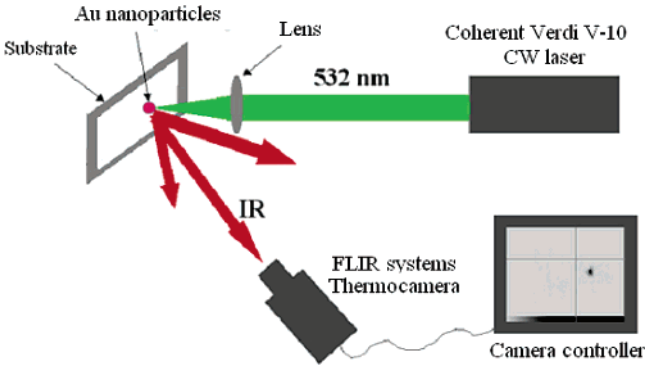

Figure 2. Schematic illustration of the IR thermographic detection of surface-bound Au nanoparticles.

between the temperature recorded before and 10 s after the laser irradiation. The measurement was performed in air, and a schematic of the experimental design is shown in Figure 2.

Atomic Force Microscopy (AFM). Atomic force micrographs were obtained on a Digital Instruments Nanoscope IIIa in tapping mode using noncontact silicon tips.

Transmission Electron Microscopy (TEM). Sample preparation for electron microscopy of the silica-coated Au NPs was accomplished by placing a 10-μL droplet of sample suspension on a Formvar-coated grid (Part no. 1820, Ted Pella) and letting the solution evaporate for >3 h. Micrographs of the silica-coated NPs were recorded with a JEOL 2010F transmission electron microscope (TEM) equipped with a high-resolution pole piece and a field emission source operated at 200 kV. Conventional bright field images were acquired with a Gatan imaging filter, which is coupled to the TEM. Digital image acquisition parameters included a scan rate of 0.5 s and final image resolution of 1024 × 1024 pixels.

DNA Detection Using Infrared Thermography. Two types of assays were performed to detect DNA hybridization: a direct assay and a sandwich assay. In the direct assay, thiol-modified target DNA strands were attached to Au NPs and were hybridized to complementary probe strands immobilized on ITO. Following hybridization, the slides were rinsed with water to wash away unbound NPs. Oligonucleotides with a length of 20 nucleotides and a hybridization temperature of 39 °C were used. The sandwich assay was implemented in the following manner: a longer target DNA strand (30 nucleotides) was hybridized both to the probe DNA strands (15 nucleotides) attached to the ITO surface and to the probe DNA strands (15 nucleotides) bound to the Au or silica-coated Au NPs. Details concerning the two assays are given below, and schematics of the experiments are presented in Figure 3.

Direct Assay. ITO slides with U20 probe DNA (NH_2-modified 20-base nucleotide, Table 1) were immersed in 900 μL of an aqueous solution containing 0.15 M NaCl, 0.015 M sodium citrate (pH 7, SSX buffer, purchased from Sigma) and ×20 modified AuNPs at the desired concentration and were allowed to hybridize at 39 °C for 7 h.

Sandwich Assay. ITO slides with NH_2-modified probe DNA (R15B, see Table 1) were immersed in 900 μL of a solution made of the desired concentration of target DNA (S30) in SSX and an excess of Au or silica-coated Au NPs modified with R15A probe DNA. The hybridization was carried out at room temperature overnight.

Following hybridization, all slides were rinsed with SSC and water and dried at 37 °C for 10 min.

RESULTS AND DISCUSSION

To improve detection limits of assays performed using nanoparticle labels and IR thermographic detection, the response of Au and silica-coated Au NPs illuminated with laser light energy tuned near the Au NP surface plasmon resonance frequency was studied. To understand the potential advantages of a silica shell, the physics of blackbody radiators are first discussed within the context of Au NP absorptions.

When Au NPs are irradiated at a frequency close to their surface plasmon resonance, they relax thermally and emit IR blackbody radiation. The amount of radiation emitted (or radiant power, W) at any frequency and temperature by a blackbody is described by Planck's law,[25]

$$W_\nu = \frac{2h\nu^3}{c^2}\frac{1}{\exp\left(\frac{h\nu}{kT}\right) - 1} \qquad \text{(i)}$$

Real objects emit only a fraction of the radiation emitted by an ideal blackbody emitter. In particular, the emissivity of real objects is defined as the ratio of the radiant power from the object to that from a blackbody at the same temperature and frequency.

$$\epsilon_\nu = \frac{W_{\nu O}}{W_{\nu b}} \qquad \text{(ii)}$$

Moreover, real materials can absorb, reflect, and transmit light. If α_ν, ρ_ν, and τ_ν are the fraction of absorbed, reflected, and transmitted light at a certain frequency, respectively, then

$$\alpha_\nu + \rho_\nu + \tau_\nu = 1 \qquad \text{(iii)}$$

For opaque materials, such as Au NPs,

$$\tau_\nu = 0 \qquad \text{(iv)}$$

and consequently,

$$\alpha_\nu + \rho_\nu = 1 \qquad \text{(v)}$$

According to Kirchoff's law, $\epsilon_\nu = \alpha_\nu$ at any specified temperature and frequency, and then, for Au NPs,

$$\epsilon_\nu + \rho_\nu = 1 \qquad \text{(vi)}$$

All metals, including Au, are highly reflective for incident radiation below the plasma frequency, and consequently, ρ_ν is quite high and ϵ_ν is close to zero (in fact, ϵ_ν for Au varies between 0.03 and 0.06, depending on surface roughness[25]). This implies that, even if Au NPs are optimal absorbers at a frequency close to their surface plasmon resonance, the low emissivity reduces the re-emitted IR radiation as a consequence of the local heating

(25) FLIR System. *ThermaCam Researcher User*'s Manual; 2004, pp 105−108.

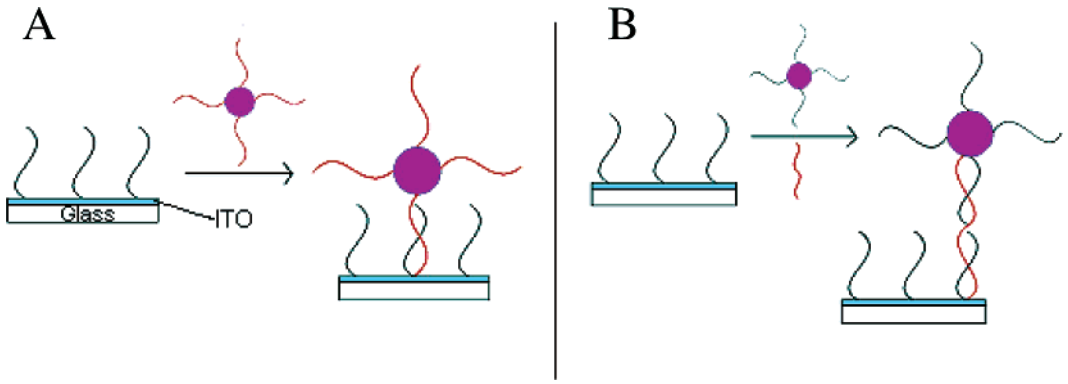

Figure 3. Schematic illustrations of DNA "direct assay" (A) and "sandwich assay" (B). Probe DNA sequences are represented in black and target DNA sequences in red. The pink spheres in A represent Au nanoparticles and in B, Au or silica-coated Au NPs.

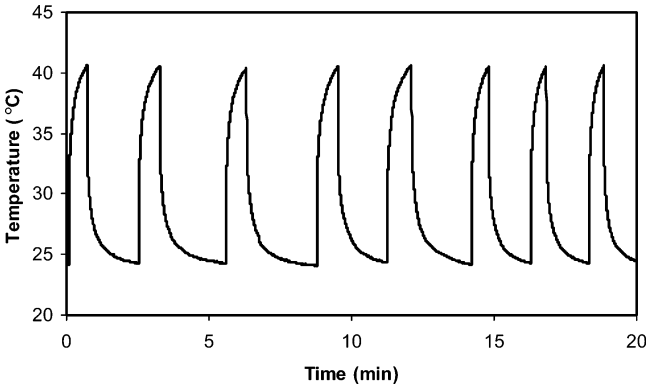

Figure 4. *T*-Jumps measured for a poly-L-lysine-coated ITO slide soaked for 30 min in a 0.5 nM Au NP solution. The laser was turned on and off every 2 min for 8 cycles.

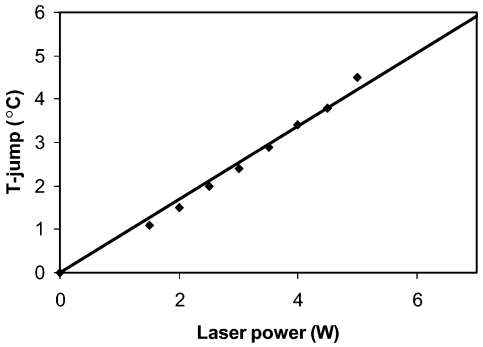

Figure 5. *T*-Jump measured on a poly-L-lysine-coated ITO slide immersed for 5 min in a 0.5 nM Au NP solution, reported as a function of laser power.

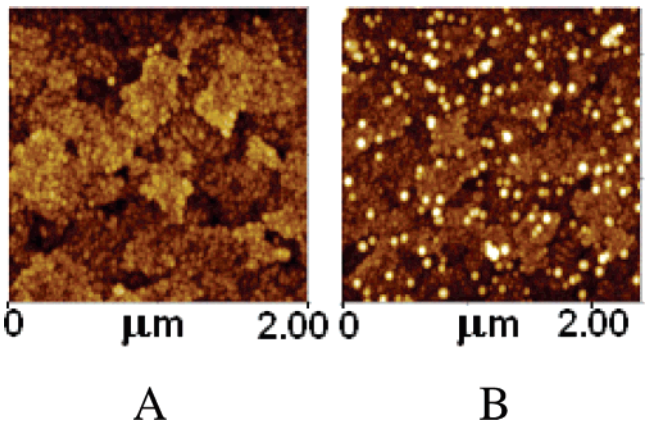

Figure 6. AFM images of an ITO slide coated with poly-L-lysine before (A) and after (B) immersion for 20 min in a 0.5 nM Au NP solution.

induced by the absorption. For this reason, in the present paper, we compare blackbody emissivity of Au NPs with the emissivity of Au NPs coated with silica, which has a very high ϵ_ν coefficient in the IR range ($\epsilon_\nu = 0.9$). The experiments reported were carried out using ITO as a substrate. ITO was chosen because it is a highly reflecting material in the IR range.[26] This means that its ρ_ν is high, and consequently, its ϵ_ν is low, according to equation vi, above. A low ϵ_ν was desirable to have low IR emission coming from the ITO background.

Temperature Jumps at ITO Slides Modified with Au NPs. Au NPs deposited on ITO slides were illuminated with laser light at 532 nm, which is not far from their surface plasmon resonance absorption.[27] To understand if the *T*-jumps recorded after illuminating Au NPs with the laser light were reproducible and proportional to the density of Au NPs, several test slides were prepared. ITO slides were coated with poly-L-lysine and immersed for 5, 15, and 30 min in 0.5 nM Au NPs solutions (see the Materials and Methods Section). The increase in temperature measured before and after 10 s of irradiation with laser light was then measured.

The measured temperature variation in response to laser light with a fluence of 1.27 W/cm^2 was found to be reproducible over eight on−off cycles, as shown in Figure 4. In this experiment, the laser light was focused on the same spot and manually turned on and off eight times over a period of about 20 min. The temperature increased to similar levels after every exposure to the laser light, thus implying that no bleaching effects occurred after laser heating. Moreover, the magnitude of the observed *T*-jumps shows a linear dependence on laser power, as shown in Figure 5. Linear signal response is highly desirable for quantitative analysis using thermographic methods. Although the response according to the Stefan−Boltzmann law is intrinsically nonlinear with the emitted flux proportional to σT^4, the response of the IR camera is calibrated so that it provides a linear temperature measurement. Figure 6 shows AFM images of an ITO slide covered with poly-L-lysine before and after coating with Au NPs. Similar images were used to determine the density of Au NPs/μm^2 on every ITO slide, and the *T*-jumps obtained after laser

(26) Brewer, S. H.; Franzen, S. *J. Alloys Compd.* **2002**, *338*, 73−79.
(27) Swanson, N. L.; Billard, B. D. *Nanotechnology* **2003**, *14*, 353−357.

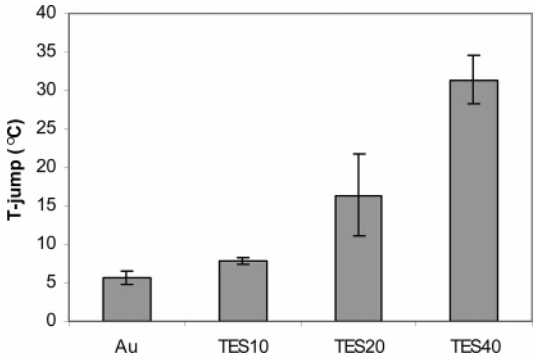

Figure 7. *T*-Jump recorded on an ITO slide after evaporation of 2-μL droplets of 2 nM solutions of 10-nm-diameter Au NPs and silica-coated Au NPs synthesized with 10, 20, and 40 μL of TES (samples TES10, TES20, and TES40, respectively). The laser fluence used was 0.5 W/cm^2.

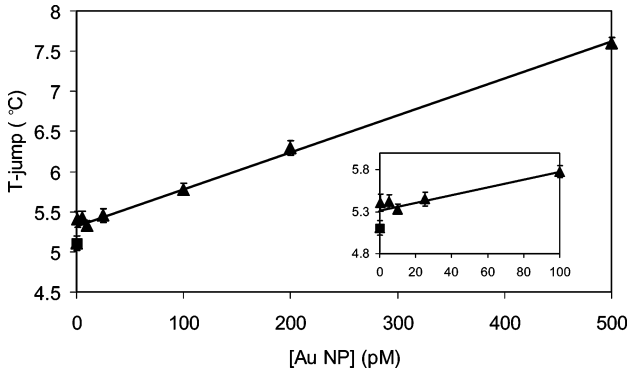

Figure 8. *T*-Jump vs Au NP concentration obtained for the direct assay. The samples represented with triangles were prepared using ITO slides covered with probe DNA (sequence U20, Table 1). The sample represented with a square was prepared using an ITO slide without probe DNA to test the nonspecific adsorption of Au NPs. Inset shows the low concentration range.

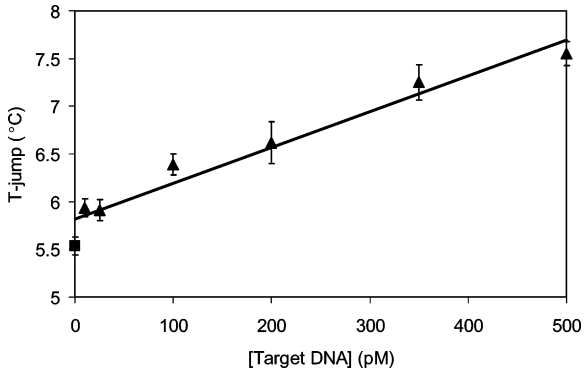

Figure 9. *T*-Jump vs target DNA (sequence S30, Table 1) concentration obtained for the sandwich assay. The sample denoted by a square was prepared without target DNA to test the nonspecific absorption of Au NPs, whereas target DNA was used for all the other samples (triangles).

irradiation were measured for each slide. It was determined that an increase in density of 10 Au NPs/μm^2 induced an increase in T jump of 1.5 °C. The limit of detection, estimated as the lowest measured Au NP density plus 3 times the SD (standard deviation) was 10 ± 3.0 particles/μm^2, that is, 1.6 ± 0.5 fmol/cm^2.

It was then of interest to determine whether DNA detection limits using IR thermography could be improved with the use of silica-coated Au NPs. Silica has a larger emissivity at the detection wavelength and, thus, should enhance the intensity of IR radiation emitted after irradiation with laser light. To test this hypothesis, silica-coated Au NPs were synthesized using increasing amounts of TES precursor (samples TES10, TES20, and TES40; see Table 2). Droplets (2 μL) of 2 nM solutions of these particles were evaporated on an ITO slide, together with a 2-μL droplet of 2 nM solution containing bare Au NPs. The *T*-jumps obtained after illuminating the slide with the 532-nm laser were measured (laser fluence = 0.51 W/cm^2). The results are shown in Figure 7. The *T*-jumps recorded were higher on the spots containing silica-coated Au NPs, as compared to the spot made of bare Au NPs. Moreover, the *T*-jumps were higher on the particles prepared with more TES. Considering that the number of Au particles was roughly the same on each spot, the differences in *T*-jumps observed must be related to differences in emissivity of the samples. This indicates that the silica shell increased the amount of IR radiation emitted by the nanoparticles irradiated with the laser.

Detection of DNA Hybridization with Au and Silica-Coated Au Nanoparticle Labels and Infrared Thermography. After finding that Au and silica-coated Au NPs irradiated with laser light at 532 nm provided intense thermographic signals, they were tested as labels in DNA hybridization assays. Two types of DNA detection assays were performed: a direct assay and a sandwich assay.[28] *T*-Jumps measured upon irradiation of a slide prepared using Au NPs labels for the direct assay are shown in Figure 8. Each data point reported is the average of at least four experiments performed under identical conditions. The results obtained show that the magnitude of the *T*-jump vs Au NP solution concentration is linear in the 0.5−500 pM range (R^2 = 0.986). As a control experiment, *T*-jumps were measured when Au NPs conjugated to DNA X20 (Au/X20 NPs) were nonspecifically bound to the surface. ITO slides covered with UDA (i.e., in the absence of DNA U20) were soaked in solutions containing varying concentrations of Au/X20 NPs. The slides were then rinsed and dried as usual. Since no U20 was present, and thus, no hybridization could occur, the particles that were not washed away were nonspecifically adsorbed on the ITO/UDA slides. This experiment simulates what would be observed in a DNA array if the target DNA strands were noncomplementary to the probe DNA strands and were nonspecifically adsorbed onto the array. The average of the results obtained in these experiments is shown as a black square on the plot. The detection limit of the assay, estimated as the mean of the control sample plus 3 times the standard deviation obtained on the control sample, was 100 pM. Since the volume of solution used for the hybridization was 900 μL, this corresponded to a total of 90 fmol of DNA-coated Au NPs.

The results obtained with Au NP labels employed in a sandwich assay are reported in Figure 9 (data corresponds to the average of three replicates). In this plot, the concentration of the target DNA (S30) is reported on the *x* axis, and the black square is the measured response in the absence of S30 target DNA due to NP nonspecific adsorption. The detection limit was 100 pM, that is, 90 fmol of target DNA.

(28) Taton, T. A.; Mirkin, C. A.; Letsinger, R. L. *Science* **2000**, *289*, 1757−1760. Taton, T. A.; Lu, G.; Mirkin, C. A. *J. Am. Chem. Soc.* **2001**, *123*, 5164−5165.

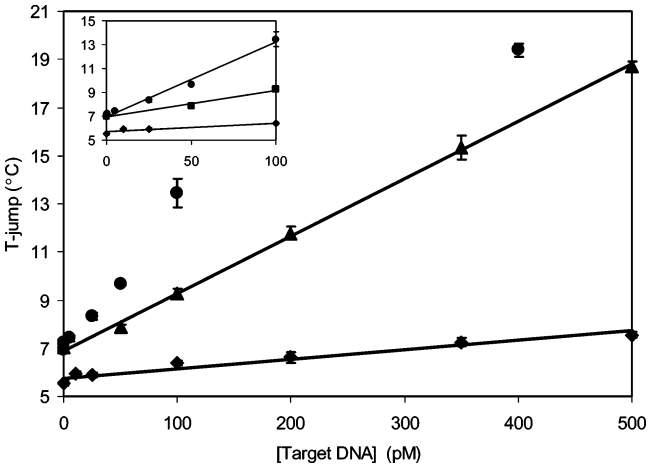

Figure 10. Sandwich assay performed with Au nanoparticles (♦), Au/SiO_2-100 (▲), and Au/SiO_2-300 (●). Inset: same data showing the 0−100 pM range.

The sandwich assay was then performed using silica-coated Au NPs as labels to test the effectiveness of the silica coating in increasing the thermographic response in a DNA hybridization detection assay. These particles were coated with probe DNA sequence R15A. The results of the assay are summarized in Figure 10, where *T*-jumps recorded for the sandwich assay performed with Au NPs are compared with those obtained with silica-coated Au NPs. To simplify, we classified the silica-coated Au NPs into two groups, depending upon the average diameter of the particles. Au/SiO_2-100 particles were 100 nm in diameter or smaller and included samples A and B (Table 2 and Figure 1), whereas Au/SiO_2-300 particles were larger, with diameters of 200−300 nm (i.e., sample C, Table 2 and Figure 1). *T*-jumps recorded for the sandwich assays performed using silica-coated Au NPs were higher than those obtained using bare Au NPs. In addition, *T*-jumps were higher for particles with a thicker silica shell (Au/SiO_2-300). *T*-Jumps increased linearly with target DNA concentration for the smaller silica-coated Au NPs (Au/SiO_2-100); however, for the larger particles (Au/SiO_2-300), a linear trend was observed only in the lower concentration range (see inset in Figure 10), whereas the *T*-jumps measured at higher concentration appeared to reach a limiting or saturation value. This may be related to the fact that the DNA-coated Au/SiO_2-300 particles were too bulky, and not all of them could hybridize to the target DNA present at high concentration on the ITO slide. Finally, Figure 10 shows that the detection limit was decreased to 10 pM (i.e., 9 fmol of target DNA) when Au/SiO_2-300 particles were used. This implies that an improvement of a factor of 10 was achieved due to the SiO_2 coating. This value approaches the detection limit of the more consolidated methods that use fluorescence labeling for target DNA or RNA probes, which usually ranges between 0.1[29] and 0.5 fmol.[30] The method described in the present paper could still be optimized, for example, by improving DNA immobilization on the ITO substrate and, thus, hybridization yield. Moreover, it could represent a viable alternative to the analysis of some biological samples that show autofluorescence, which would interfere with the detection of fluorescent-labeled target molecules.[31]

CONCLUSIONS

The blackbody radiation emitted by Au and silica-coated Au nanoparticles under laser irradiation was studied as an observable trait for sensing applications. The particles were irradiated with laser light at a frequency close to the surface plasmon resonance of Au, and the re-emitted blackbody radiation was detected with an IR camera equipped with an InAs array detector. The particles were deposited on an indium tin oxide (ITO) substrate. Proof-of-principle experiments carried out using Au NPs showed that the temperature jumps measured as a difference between the temperature recorded before and after laser irradiation were directly proportional to the number of Au NPs present on the ITO slide. Moreover, it was shown that the *T*-jumps were reproducible and directly proportional to the laser power. The limit of detection was 1.6 fmol of Au NPs/cm^2. Au NPs were then coated with a silica layer to increase their IR emissivity. *T*-Jumps recorded upon irradiation of these NPs deposited on ITO were, indeed, higher than those measured with bare Au NPs. Moreover, when more silica precursor was used, particles with thicker silica shells were obtained, and it was observed that the *T*-jumps upon laser irradiation were higher on the particles with thicker shells. This implied that coating Au NPs with silica indeed increased particle emissivity.

Both Au and silica-coated Au NPs were then coated with DNA and tested as labels for two types of hybridization detection assays (direct and sandwich assay). A detection limit of 100 pM was achieved for both assays with the Au NPs, whereas target DNA concentrations as low as 10 pM could be detected in the sandwich assay when silica-coated Au NPs were used. Under the conditions of the experiment, these concentrations correspond to a total amount of 90 and 9 fmol of target DNA, respectively. These results show that thermographic detection of blackbody radiation emitted by Au NPs can be successfully used to develop a sensitive detection assay and that the detection limit can be lowered by coating the Au NPs with a silica layer.

ACKNOWLEDGMENT

The authors thank Drs. Timothy Woudenberg and Ben Schroeder at Applied BioSystems for discussions and financial support.

Received for review January 9, 2006. Accepted March 20, 2006.

AC0600555

(29) Lockhardt, D. J.; Dong, H.; Byrne, M. C.; Follettie, M. T.; Gallo, M. V.; Chee, M. S.; Mittmann, M.; Wang, C.; Kobayashi, M.; Horton, H.; Brown, E. L. *Nat. Biotechnol.* **1996**, *14*, 1675−1680.

(30) Duggan, D. J.; Bittner, M.; Chen, Y.; Meltzer, P.; Trent, J. M. *Nat. Genet. Suppl.* **1999**, *21*, 10−15.

(31) Blab, G. A.; Cognet, L.; Berciaud, S.; Alexandre, I.; Husar, D.; Remacle, J.; Lounis, B. *Biophys. J.* **2006**, *90*, L13−L15.